doi: 10.15407/ujpe61.11.0960

O.V. SOLOMENKO,[1] O.V. PRYSIAZHNA,[2] V.YA. CHERNYAK,[2] V.V. LENDIEL,[2]
D.K. HAMAZIN,[2] EU.V. MARTYSH,[1] D.O. KALUSTOVA,[1] I.V. PRYSIAZHNEVYCH[1]

[1] Taras Shevchenko National University of Kyiv,
Faculty of Radio Physics, Electronics, and Computer Systems
(64/13, Volodymyrs'ka Str., Kyiv 01601, Ukraine; e-mail: oksana_solomenko@ukr.net)
[2] Taras Shevchenko National University of Kyiv,
Faculty of Radiophysics, Electronics, and Computer Systems
(64/13, Volodymyrs'ka Str., Kyiv 01601, Ukraine)

INVESTIGATION OF A MICRODISCHARGE SYSTEM WITH THE VORTEX GAS FLOW

PACS 52.50.Dg; 52.80.-s

A microdischarge system has been studied with the use of various plasma gases. The results of emission spectroscopy and measurements of the current-voltage characteristics are reported. The discharge parameters for the vibrational and rotational levels of plasma components are determined.

K e y w o r d s: microdischarge, vortex flow, optical emission spectroscopy.

1. Introduction

Nowadays, the generation of microdischarge plasma can be considered as one of the most promising directions in non-equilibrium plasma chemistry. A considerable number of works are devoted to this subject [1], because the application of microdischarge plasma is promising for the low-temperature treatment of materials. A number of devices have already been developed, which are intended for the treatment of oral cavity (e.g., dental bleaching [2], the improvement of the filling material density, mouth treatment [3–5], and others). There are also experimental data testifying to a possibility of successfully using plasma to treat living tissues in order to deactivate microorganisms [6], for sterilization [7], inactivation of cancer cells [8], to stop bleeding (for blood coagulation), to heal wounds, and so on. A challenging problems are the treatment of surfaces using microdischarges, the deposition of films with required properties – e.g., wetting [9] – on the surface, *etc.* Microdischarges are also actively used for the creation of C–C and C–N bonds and the conversion of C_2H_8 in micro-reactors [10,11]. All those applications become feasible, because low-power microdischarges ($\leq$10 W) allow plasma flows with a low energy and a high non-equilibrium level to be generated.

Owing to their properties, microdischarges can be used as sources of chemically active components. It was shown that the application of plasma together with known medical methods substantially improves treatment efficiency. The combination of active coatings as a source of particles on the walls of microdischarge devices with additional activation of the surface by plasma can be used to obtain chemical products in a power-efficient way [10].

In medicine, the interest in various microplasma systems is associated with their ability to generate low-temperature non-equilibrium plasma at atmospheric pressure. As a rule, the temperature of electrons in this plasma is sufficient for the initiation of many chemical reactions: modification of DNA, proteins, and cell membranes, and the generation of radicals [10]. At the same time, the temperature of the heavy plasma component (ions and neutrals) is close to room one in this case. Therefore, the process of plasma treatment does not destroy biological tissues, which are sensitive to the temperature. The processes of disinfection, deactivation, and sterilization with the participation of active plasma particles (radicals, charged particles, excited particles, UV radiation) run rather quickly. Experiments showed that, in order to neutralize viruses and bacteria of various types on the surface and in aqueous solutions,

the corresponding plasma treatment within a time interval from a few seconds to several minutes is required [12].

At present, there are two basic approaches to the application of low-temperature plasma at the atmospheric pressure for disinfection, deactivation, and sterilization. In the first approach, plasma is generated in a discharge interval; afterward, the generated products are transported by a gas flow to treated biological tissues. The majority of charged particles disappear beyond the region of plasma generation. Therefore, the therapeutic effect may expectedly be provided by long-living neutral particles and radicals. The application of described plasma sources ensures a point-like action on the alive tissue surface.

In the second approach, plasma is generated at a direct contact with the alive tissue. In this case, the biological tissue directly serves as one of the electrodes [13]. This approach is considerably different from the previous one. First, plasma is in a direct contact with the biological surface, which provides both a possibility of the surface charging and the delivery of high-energy ions. Another feature consists in that the strength of the electric field created at the surface [14] is much (many orders of magnitude) higher than in the case of indirect contact with plasma. Hence, depending on a specific purpose, that or another approach is applied. Usually, rare gases such as helium or argon are used to avoid a plasma instability. For this aim, the discharge is doped with molecular gases, such as oxygen, with concentration of few percents [14].

Nowadays, plenty of devices have been developed for the generation of microplasma jets. They are based on different discharge types: barrier, corona, glow, HF, and others. However, for the majority of them, a high voltage (about several kilovolts) is required, which is too high for medical applications. As a result, the safety of plasma systems with respect to alive biological objects decreases. Therefore, microdischarges can be rightly regarded as one of the most promising generators of low-voltage plasma jets for the application in biomedicine. Depending on the working gas, they can be applied at considerably lower voltages of discharge supply: ($U \approx 300$ V).

In this work, the results of researches carried out on an original microdischarge plasma system with a vortex gas flow are reported. The application of a vortex gas flow can prolong the operating time of the system due to a reduction of the electrode destruction under the plasma action and can stabilize the plasma jet in space. Moreover, one may expect to obtain the temperature of the heavy plasma component that is typical of glow discharges and substantially diminishes the geometrical dimensions of the electrode system.

2. Experimental Setup

In Fig. 1, *a*, the schematic diagram of the experimental setup for the measurements of the electric parameters of microdischarges and the optical parameters of plasma generated by a microdischarge jet is shown. The microdischarge generator (Fig. 1, *b*) was an axially symmetric system with water-cooled internal electrode (1). This electrode was insulated from the case by means of dielectric tube (4). The working gas (air, Ar, or CO_2) was blown in tangentially to the lateral surface through aperture (2). The aperture diameters were $d = 0.5$, 1.0, 1.5, or 2.0 mm, and the gas flow $G = 1.5$ or 3.0 l/min. Copper electrodes (3) were arranged at a distance of 1 mm from each other. The internal electrode was fabricated in the form of a wire 1 mm in diameter, and the external one was a plate with a thickness of 1 mm. A BP-138 power unit with a positive potential and a BP-100 one with a negative potential were used as sources of high-potential power supply. The external electrode was always grounded.

3. Experimental Results

In this work, the current-voltage characteristics (CVCs) of the device described in the previous section were measured in the current interval from 2 to 60 mA, and the parameters of microdischarge plasma were studied.

In Figs. 2 and 3, the results of microdischarge CVC measurements are depicted. They were obtained at various polarities of the high-voltage electrode and at various diameters d of the output aperture, from which the discharge jet was blown out. The corresponding value of gas flow was $G = 1.5$ l/min. The maxima of experimental points in the CVCs correspond to the relevant breakdown voltages. It should be noted that increase of the output aperture diameter gave rise to shorter microplasma jet lengths. It was found that the discharge burning voltages were higher, if the potential of the high-voltage electrode was positive.

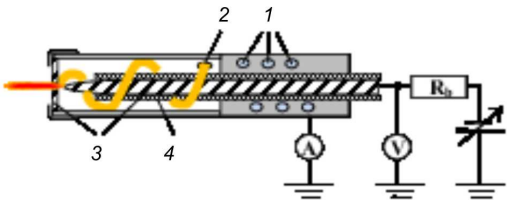

a

b

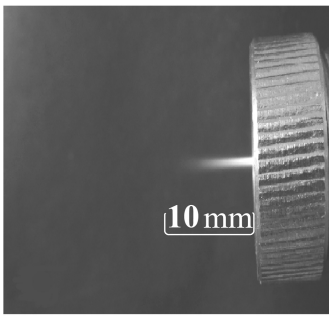

c

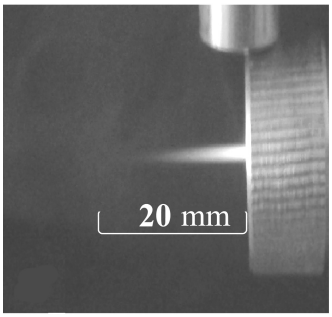

d

Fig. 1. Schematic diagram of the microdischarge generator (*a*), photo image of the assembled construction (*b*), and photo images of a discharge jet, when air (*c*) or CO_2 (*d*) is used as a working gas

As is evident from the presented CVCs, the voltage drop across the discharge decreased with the reduction of *d*. Figures 2 and 3 testify that the discharge burning voltage decreased as the plasma gas was varied: $C_2 \rightarrow$ air $\rightarrow$ Ar. One can also see that the microdischarge CVCs are similar to those of the low-pressure gas discharge, which have sections of the normal glow discharge (at about 10 mA and above). At lower currents, the curves have a section that reminds a subnormal glow discharge.

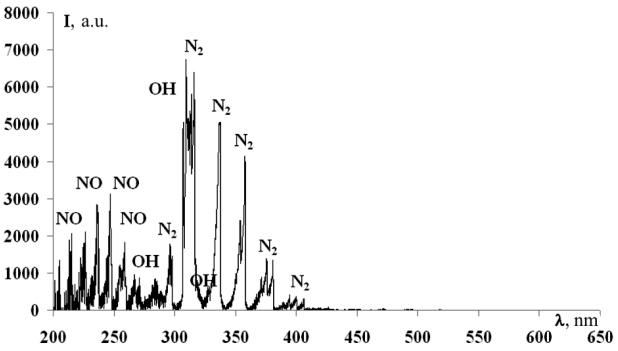

Fig. 2. Typical emission spectrum of microdischarge plasma in a wavelength interval of 200–650 nm. The discharge current $I = 30$ mA, $U = 1200 \div 1300$ V, $G(\text{air}) = 3$ l/min, the output aperture diameter $d = 2$ mm, the interelectrode distance $l = 1$ mm, $h = 2.5$ mm

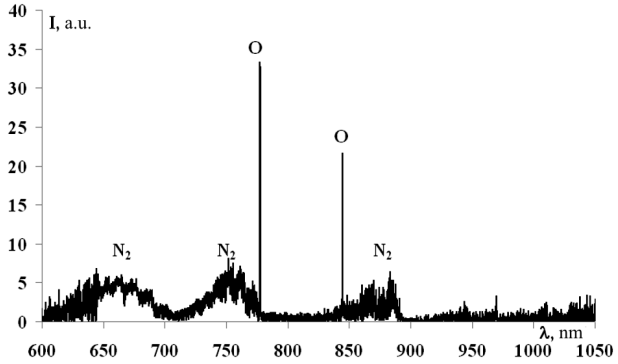

Fig. 3. The same as in Fig. 2, but for a wavelength interval of 600–1050 nm

To study the discharge behavior in various regimes, photo and video registration methods were used. They allowed us to notice that when the gas was changed ($C_2 \rightarrow$ air $\rightarrow$ Ar), the length of the microdischarge jet became shorter (see Figs. 1, *c* and *d*). In the case where Ar was used, the jet did not exceed 2–3 mm. Taking into account that the electrode with the aperture was pressed with the help of a special attachment 2.0 mm in thickness, the spectrum of microdischarge plasma was measured along the plasma jet starting from a distance of 2.5 mm.

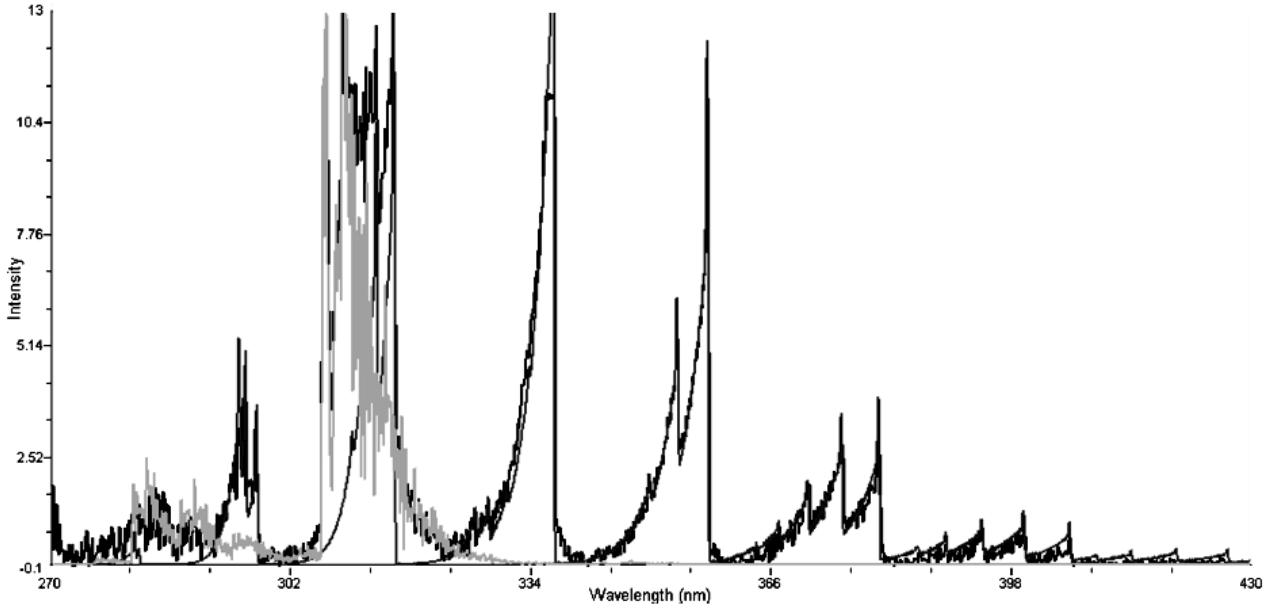

Fig. 4. Comparison of the experimental emission spectrum of microdischarge plasma (black curve) with the simulations for nitrogen N_2 (C-B) (gray curve) and hydroxyl OH (A-X) (light gray curve) at $T_r^*(N_2) = T_r^*(OH) = 2500 \pm 500$ K and $T_v^*(N_2) = T_v^*(OH) = 4500 \pm 500$ K. The discharge current $I = 30$ mA, $U = 1200 \div 1300$ V, G(air) $= 3$ l/min, the output aperture diameter $d = 2$ mm, the interelectrode distance $l = 1$ mm, $h = 2.5$ mm

The plasma components were analyzed, and the plasma parameters were studied with the use of plasma emission spectroscopy. The spectra were registered on an S-150-2-3648 USB spectrometer on the basis of the Solar TII CCD rule. The latter operates in a wavelength interval of 200–1080 nm and has a triangular instrument function with a halfwidth of 0.2 nm in a wavelength interval of 200–650 nm and 0.3 nm in an interval of 650–1080 nm. Radiation in the direction perpendicular to the plasma jet axis was registered.

In Figs. 4 and 5, a typical emission spectrum of microdischarge plasma measured at the distance $h = 2.5$ mm from the surface of the external electrode is shown. The spectrum was registered at the following experimental parameters: the discharge current $I = 30$ mA, the voltage $U = 1200 \div 1300$ V, the output aperture diameter $d = 2$ mm, and the interelectrode distance $l = 1$ mm. The intensity of working gas (air) supply amounted to $G = 3$ l/min. The corresponding length of the visible part of the microdischarge plasma jet reached 8 mm. As one can see from the figures, the main fraction of radiation was emitted in the UF spectral range, in a wavelength interval of 200–430 nm (Fig. 4). It was much more intense than the spectrum fraction within an interval of 600–1000 nm (Fig. 5).

It is evident that the spectra are complicated and multicomponent. At the same time, they contain only the components of a working gas, namely, the atomic multiplets of oxygen (O: 777 and 844 nm), the molecular bands of hydroxyl (OH) and NO, and the bands of the first (Fig. 5) and second (Fig. 4) positive systems of nitrogen (N_2). It should be noted that the emission intensity decreased along the jet, but the form of the spectrum remained invariant within the measurement error, which testifies that the component ratios and the parameters of plasma also remained invariant along the plasma jet.

The characteristic temperatures corresponding to the excited states of atomic and molecular (the temperatures of excited vibrational, T_v^*, and rotational, T_r^*, levels) components were determined, by using various methods of emission spectroscopy. The following basic assumptions were used while simulating the emission spectra of molecules (the software code SpecAir [15]):

• the distributions over the rotational and vibrational levels of the excited and ground electron levels are identical,

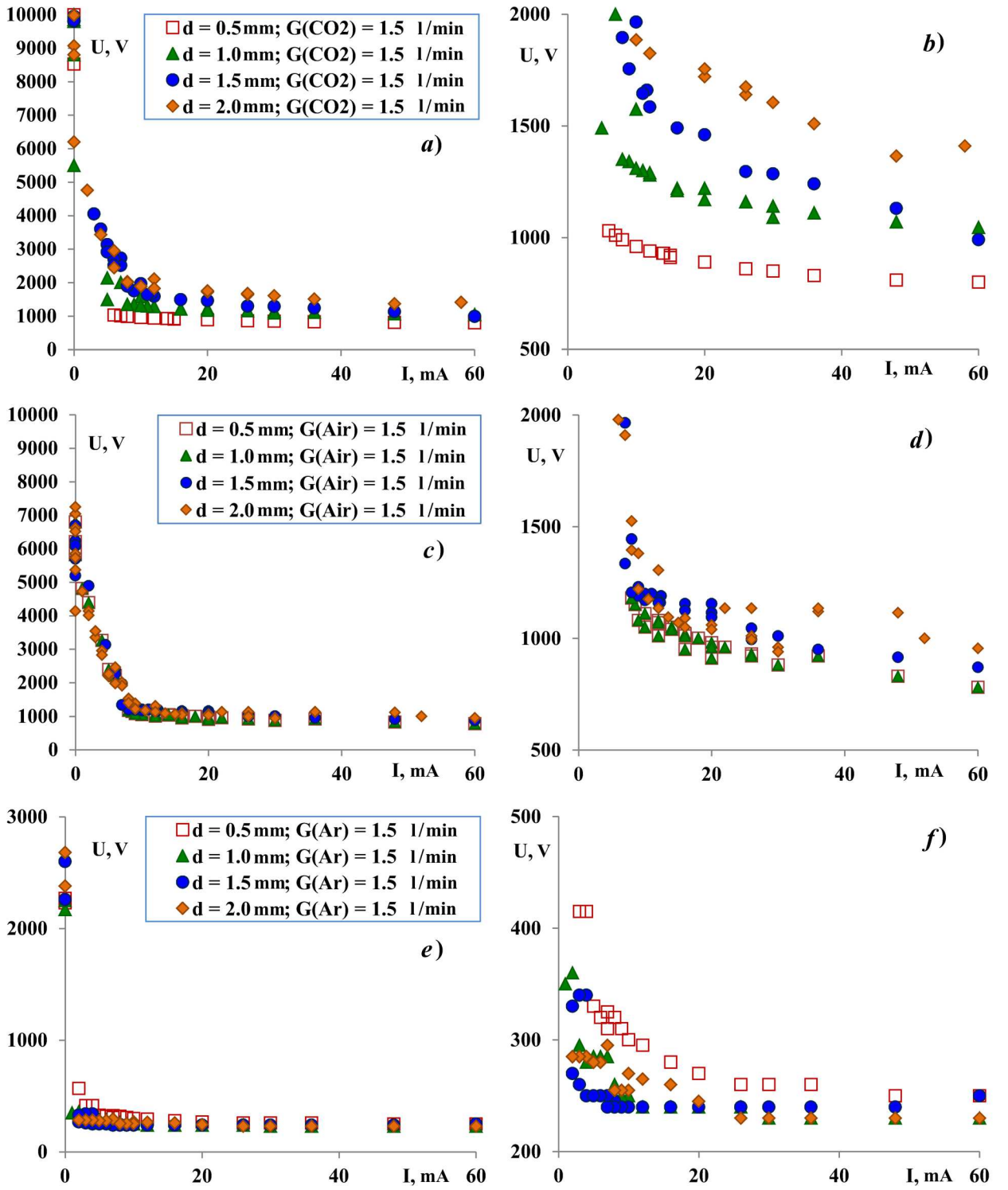

Fig. 5. Experimental current-voltage characteristics measured in the CO_2 (*a* and *b*), air (*c* and *d*), and Ar (*e* and *f*) flows ($G = 1.5$ l /min) at the positive polarity of the high-voltage electrode and various *d*

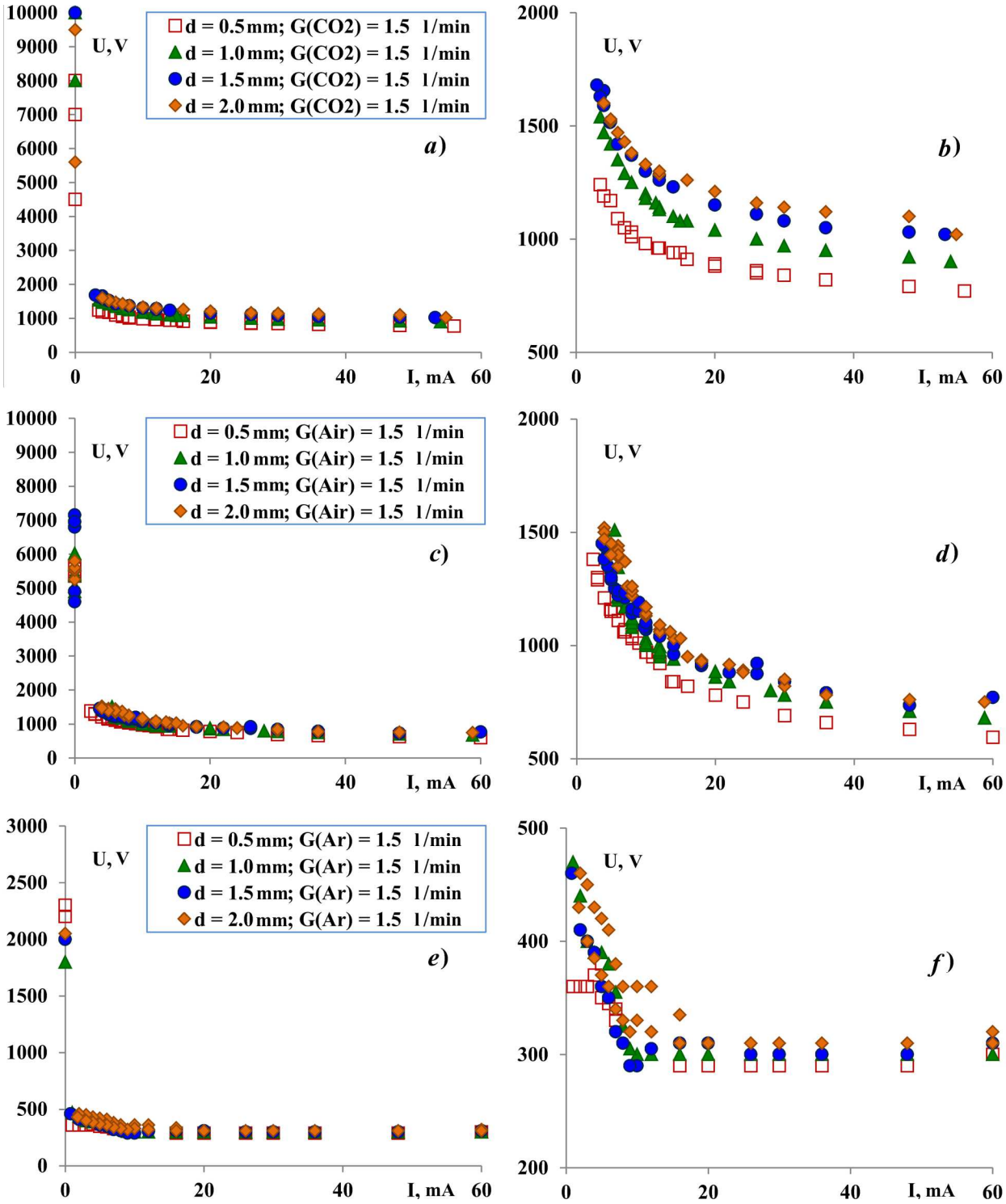

Fig. 6. Experimental current-voltage characteristics measured in the CO_2 (*a* and *b*), air (*c* and *d*), and Ar (*e* and *f*) flows ($G = 1.5$ l /min) at the negative polarity of the high-voltage electrode and various d

• the distributions over the rotational and vibrational levels correspond to the Boltzmann distributions with the corresponding T_v^* and T_r^* [15],

• the rotation temperature equals the gas one.

Special attention was paid to molecular bands, which did not overlap. They corresponded to transitions from an excited electron state into the ground one. As was already demonstrated in the OH case, those states in the gas-discharge plasma at the atmospheric pressure are characterized by the Boltzmann distribution over the rotational levels, and the temperature T_r^* of the excited electron level is close to the gas temperature [16]. Those states make a substantial contribution to the spectrum excitation by means of the direct electron impact [17].

The discharge temperatures for the excited vibrational and rotational levels of molecules were determined by comparing the experimentally measured spectra containing unresolved rotational bands and the radiation emission spectra of nitrogen (N_2) and hydroxyl (OH) molecules synthesized by the software code Specair. In Fig. 6, the example of a comparison between the experimental spectrum (the black curve) and the simulation results for N_2 ($C^3\Pi_u$-$B^3\Pi_g$) (the gray curve) and OH ($A^2\Sigma^+$-$X^2\Pi_i$) (the light-gray curve) is illustrated. The simulation temperatures were selected identical for both components: $T_r^*(N_2) = T_r^*(OH) = 2500 \pm 500$ K, $T_v^*(N_2) = T_v^*(OH) = 4500 \pm 500$ K.

We managed to register only two highly intensive multiplets of atomic oxygen in the spectra, namely, at 777 and 844 nm. Therefore, since the energies of those multiplets are close to the upper energy levels, we failed to determine the occupation temperature for the excited electron levels, $T_e^*(O)$.

To summarize, it was shown in this work that

• in the examined current interval, the discharge voltage depends on the nature of a plasma-forming gas; in particular, for the row $CO_2 \rightarrow$ air $\rightarrow$ Ar, the discharge burning voltage decreases;

• the intensity of gas flow weakly affects the discharge burning voltage in the examined current interval;

• the increase of the aperture diameter in the output electrode gave rise to the growth of the discharge burning voltage;

• as the plasma gas was changed ($CO_2 \rightarrow$ air $\rightarrow$ Ar), the length of plasma jet decreased;

• microdischarge plasma is non-isothermal, and the ratios between its components remains invariable along the plasma jet; the emission intensity increases with the distance along the jet.

1. K.H. Becker, K.H. Schoenbach, J.G. Eden. Microplasmas and applications. *J. Phys. D: Appl. Phys.* **39**, R55 (2006) [DOI: 10.1088/0022-3727/39/3/R01].
2. S.H. Nam, H.W. Lee, S.H. Cho *et al.* High-efficiency tooth bleaching using non-thermal atmospheric pressure plasma with low concentration of hydrogen peroxide. *J. Appl. Oral Sci.: Revista FOB* **21(3)**, 265 (2013) [DOI: 10.1590/1679-775720130016].
3. A.C. Ritts, H. Li, Q. Yu *et al.* Dentin surface treatment using a non-thermal argon plasma brush for interfacial bonding improvement in composite restoration. *Eur. J. Oral Sci.* **118(5)**, 510 (2010) [DOI: 10.1111/j.1600-0722.2010.00761.x].
4. G.C. Kim, H.W. Lee, J.H. Byun *et al.* Dental applications of low-temperature nonthermal plasmas. *Plasma Process Polym.* **10**, 199 (2013) [DOI: 10.1002/ppap.201200065].
5. Y. Liang, Y. Li, K. Sun *et al.* Plasma thorns: Atmospheric pressure non-thermal plasma source for dentistry applications. *Plasma Process Polym.* **12**, 1069 (2015) [DOI: 10.1002/ppap.201400185].
6. J. Mizeraczyk, M. Dors, M. Jasiński *et al.* Atmospheric pressure low-power microwave microplasma source for deactivation of microorganisms. *Eur. Phys. J. Appl. Phys.* **61**, 24309 (2013) [DOI: 10.1051/epjap/2012120405].
7. H.S. Uhm, E.H. Choi, G.S. Cho. Sterilization of microbes by using various plasma jets. *J. Korean Phys. Soc.* **60**, 897 (2012) [DOI: 10.3938/jkps.60.897].
8. A.A. Fridman, G. Friedman. *Plasma Medicine* (Wiley, 2013).
9. R.F. Caetano, Y.D.U. Hoyer, C. Oliveira *et al.* Study of microhollow cathode glow discharge to improve the wettability on surface of polypropylene film. *Am. J. Cond. Matter Phys.* **4**(3A), 32 (2014) [DOI: 10.5923/s.ajcmp.201401.05].
10. A. Agilar, *PhD thesis* (2009).
11. T. Nozaki, K. Okazaki. Plasma enhanced C_1-chemistry: towards greener methane conversion. *Green Process Synth.* **1)**, 517 (2012) [DOI: 10.1515/gps-2012-0074].
12. J.A. Daseco, K.G. Pabeliña, Ma.A.T. Siringan *et al.* Comparative study on the use of different metal electrodes in low-pressure glow discharge plasma sterilization. *Plasma Medicine* **4**, 1 (2014) [DOI: 10.1615/ PlasmaMed.2014011720].
13. N.Y. Babaeva, M.J. Kushner. Intracellular electric fields produced by dielectric barrier discharge treatment of skin. *J. Phys. D: Appl. Phys.* **43**, 185206 (2010) [DOI: 10.1088/0022-3727/43/18/185206].
14. N.Yu. Babaeva, M.J. Kushner. Reactive fluxes from atmospheric pressure plasmas for deactivation of bacteria on

rough surfaces and suspended in air. *Proc. 20th Int. Symp. Plasma Chemistry* (2011).

15. C.O. Laux. Radiation and Nonequilibrium Collisional-Radiative Models. In *Physico-Chemical Models for High Enthalpy and Plasma Flows* (von Karman Institute for Fluid Dynamics, 2002).
16. V.I. Arkhipenko, A.A. Kirilov, Y.A. Safronau *et al.* DC atmospheric pressure glow microdischarges in the current range from microamps up to amperes. *Eur. Phys. J. D* **60**, 455 (2010) [DOI: 10.1140/epjd/e2010-00266-5].
17. V.N. Ochkin. *Spectroscopy of Low Temperature Plasma* (Fizmatlit, 2010) [in Russian].

Received 20.11.15

О.В. Соломенко, О.В. Присяжна,
В.Я. Черняк, В.В. Лендел, Д.К. Гамазін,
Є.В. Мартиш, Д.О. Калустова, І.В. Присяжневич

ДОСЛІДЖЕННЯ МІКРОРОЗРЯДНОЇ СИСТЕМИ З ТАНГЕНЦІАЛЬНОЮ ПОДАЧЕЮ ГАЗУ

Р е з ю м е

Проведено дослідження мікророзрядної системи за використання різних плазмоутворюючих газів. Представлено результати по виміряних вольт-амперних характеристиках та емісійної спектроскопії. Визначено параметри заселення збуджених коливальних та обертальних рівнів компонент плазми.